Engineering Structures 275 (2023) 115277

Contents lists available at ScienceDirect

Engineering Structures

journal homepage: www.elsevier.com/locate/engstruct

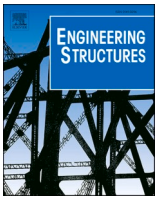

Numerical analysis of precast concrete segmental bridge decks

Javier Cañada Pérez-Sala *, Ana M. Ruiz-Teran

Imperial College London, Department of Civil and Environmental Engineering, Imperial College Road, SW7 2AZ London, United Kingdom

ARTICLE INFO

Keywords:
Precast concrete
Segmental
Bridges
External prestressing
Finite element model

ABSTRACT

Precast Concrete Segmental Bridges are nowadays a well-established alternative for bridge construction that presents significative advantages related to the construction process. Numerous bridges have been built using this technology in the past decades and extensive research has been conducted, including the development of different numerical models to study their behaviour. This paper proposes a new Finite Element model for Precast Concrete Segmental Bridge decks capable of reproducing the main characteristics of their behaviour at a reduced computational cost.

The model proposed has shown very good agreement with experimental results existing in the literature. After calibration, the influence of different modelling choices has been analysed. The results point out to a high impact of the modelling strategy adopted for the joints in the compression areas, requiring an adequate estimation of the point of contact between the segments. Additionally, consideration of friction of external tendons at the deviators showed limited relevance in the global behaviour of the model but was important for the correct estimation of stress increments in the tendons. Finally, considering or not the presence of epoxy at the joints did not seem to influence significantly the behaviour of the models. The use of shell elements combined with the modelling strategy adopted for the joints offers better accuracy than existing models with a significantly lower computational time.

1. Introduction

Precast Concrete Segmental Bridges (PCSBs) constitute an efficient and fast alternative for bridge construction that has been widely used in the past decades [1,2]. The structural behaviour of the deck in this type of bridges is conditioned by the presence of joints between the segments where the steel reinforcement is interrupted [3]. Additionally, PCSBs have been intimately linked to the use of external prestressing since its first developments [4]. Durability problems associated with internal prestressing, which resulted in a ban of its use in the UK [5], favoured external prestressing. However, the current trend in the construction of these bridges is to include both external and internal bonded tendons [6]. Extensive research has been conducted to study the influence of the joints and the prestressing on the behaviour of PCSBs and numerous analytical and numerical models have been proposed to aid in their design.

Ramos and Aparicio [7] developed a numerical model for PCSBs with fibre beam elements. They used unreinforced concrete elements between the segments whose cracking simulated the opening of the joints. More recently, Yan et al. [8] updated this model to include the effects of shear-lag and improved the joint model by dissociating its behaviour from the length of the plain concrete element. The resulting model combines efficiency, due to all the elements being one-dimensional; and accuracy, shown in the good agreement obtained with experimental results.

Veletzos and Restrepo [9] studied PCSBs with bonded tendons subjected to earthquake loads using Finite Element (FE) models with one-dimensional elements. They modelled the joints with multiple truss elements in the thickness of the web and flanges. Additionally, they conducted tests to examine the behaviour of bonded tendons through the joints and proposed including an equivalent unbonded length for internal tendons at the joints [10].

Turmo et al. [11] created two-dimensional FE models of precast segmental beams with dry joints and validated them with experimental tests. Turmo et al. studied the influence of including the shear keys at the joints in the model. They also analysed the impact of considering the

Abbreviations: PCSB, Precast Concrete Segmental Bridge; SES, Second Stage Expressway System Bangkok; CEBTP, Centre d'Études du Bâtiment et des Travaux Publiques; HDPE, High Density Polyethilene.

* Corresponding author.
E-mail addresses: j.canada-perez-sala18@imperial.ac.uk (J. Cañada Pérez-Sala), a.ruiz-teran@imperial.ac.uk (A.M. Ruiz-Teran).

https://doi.org/10.1016/j.engstruct.2022.115277
Received 12 July 2022; Received in revised form 9 October 2022; Accepted 6 November 2022
Available online 17 November 2022

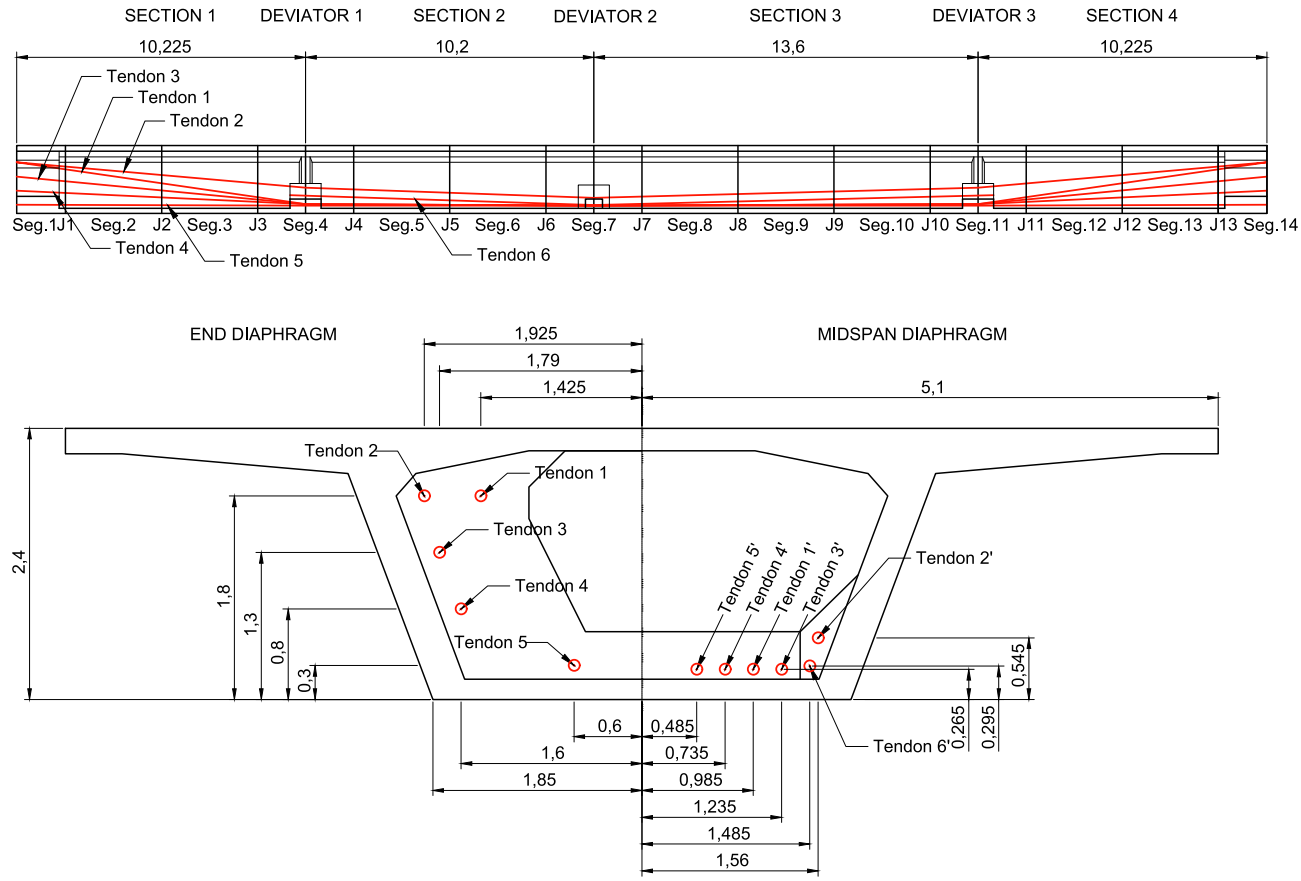

Fig. 1. Longitudinal (top) and cross (bottom) sections of the test span of the SES Bangkok.

diagonal cracking observed in the tests. They found that modelling the joints with flat surfaces only generated small differences with respect to a model where the detailed profile of the joint was considered. Additionally, Turmo et al. stated that modelling the diagonal cracking observed in the experiments allowed to better reproduce the behaviour and stiffness of PCSBs but did not seem to affect their flexural strength [12].

Although the previous models have been shown to provide good estimations of the behaviour of PCSBs while remaining computationally efficient, more complex models are required to reproduce their full spatial behaviour. In this context, Specker and Rombach [13] developed 3D FE models using shell elements for PCSBs with dry joints to study their behaviour under shear and torsion. To validate their models they compared their results to those of the experiment conducted by Takebayashi et al. [14] on a test span of the Second Stage Expressway System (SES) in Bangkok.

Specker and Rombach [13] compared models that used solid elements to reproduce accurately the profile of the joints including the shear keys, and simpler models in which the contact at the joints happened between flat shell edges. Using these models, they found that the contribution of the shear keys in transferring shear through the joints is small when the joints open at midspan, whereas it becomes more relevant at the joints close to the supports in continuous bridges.

Yuen et al. [15] also developed a 3D FE model of the test span studied by Takebayashi et al. [14] using solid elements. This model reproduced the detailed geometry of the shear keys and included the effect of friction of the external tendons at the deviators using springs. Yuen et al. used this model to evaluate the influence of the initial prestressing force. Halder et al. [16] used the same model to investigate the effects of the deck slenderness and proposed expressions to obtain the stress increments in external tendons. Halder et al. described three types of behaviour at failure depending on the initial prestressing force.

Several other proposals to model the behaviour of PCSBs can be found in the literature [17–24]. With very few exceptions [15,17], most of the existing models for PCSBs do not reproduce the friction-slip behaviour of the external tendons at the deviators, which has a relevant impact on the stresses measured in these tendons. This topic, however, has been studied in depth by other researchers for monolithic girders [25,26].

The simplest models for PCSBs [8,9,11] provide good estimations at a low computational cost, but do not capture the spatial characteristics of PCSBs. On the other hand, the most complex models using 3D solid elements [15,20,22,24] can provide excellent precision for most aspects of the behaviour of PCSBs but at a very high computational cost. This, with the computational resources commonly available, prohibits their use for computationally demanding simulations such as dynamic analyses of large models.

Thus, there is a need for a model that is capable of reproducing the 3D behaviour of PCSBs, accounting for the behaviour of joints and the prestressing, and at a reasonable computational cost that allows for its use in large and demanding analyses. An efficient model with these characteristics would allow opening new lines of research for PCSBs where dynamic effects govern the behaviour such as in railway bridges or footbridges.

Three-dimensional models using shell elements, as those proposed in [13,18,19,23], can provide a good balance between accuracy and computational cost. However, it should be possible to further improve the accuracy of this type of models, bringing it closer to the most complex models using 3D solid elements. To achieve this, improved models for the joints are needed, and the effect of friction of the external tendons at the deviators should be incorporated in the models. Moreover, the scope of the models available in the literature can be extended if the

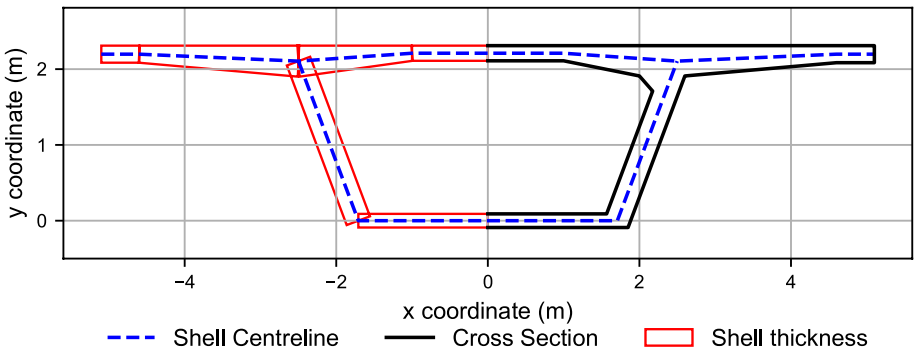

Fig. 2. Real and modelled thickness of the top and bottom flanges and webs for the test span. Model overlaps and gaps due to the modelling are also represented.

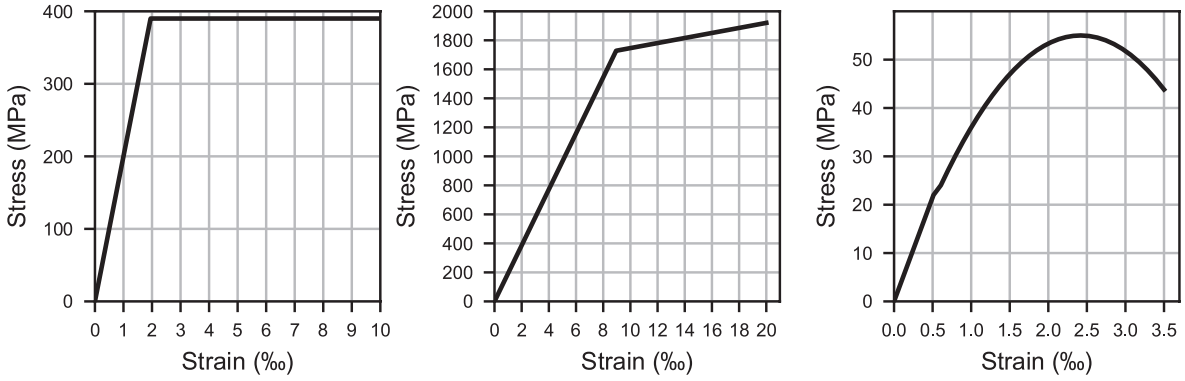

Fig. 3. Strain-stress laws for reinforcement steel (left), prestressing steel (centre) and concrete (right).

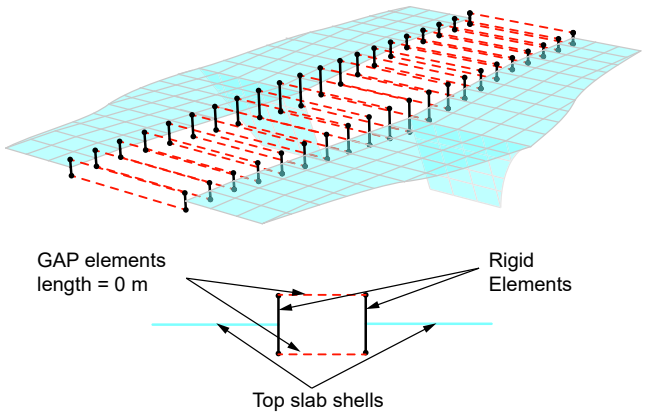

Fig. 4. Modelling strategy for the joints at the top slab with rigid elements connecting to eccentric contact elements (GAP) with null length above and below the slab.

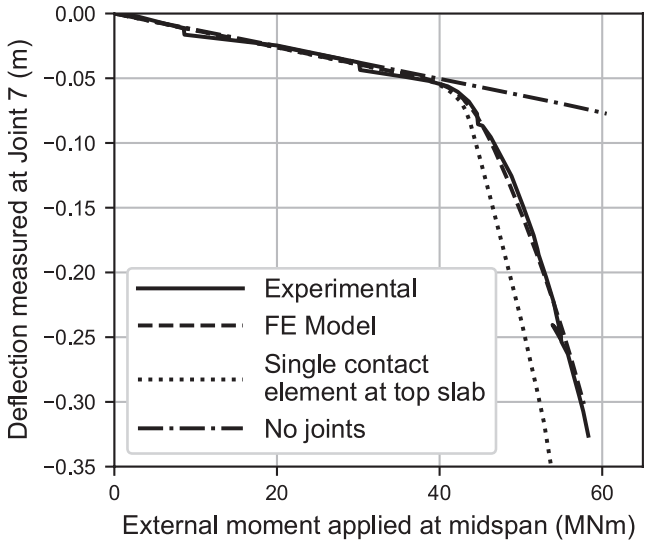

Fig. 5. Comparison of the deflection of the test span obtained from the experimental results [14], the proposed FE model, a simpler model with a single contact element at top slab at the joints, and a model with no joints between the segments.

effects of combining external unbonded tendons and internal bonded tendons and the influence of the presence of epoxy at the joints are considered.

The rest of this paper is dedicated to describing a proposal for a model that incorporates all these aspects, presenting first the modelling approaches used for its development, followed by the validation of the proposed model through comparison with experimental results in the literature. Finally, the calibrated model is used to analyse the influence of certain relevant parameters on the behaviour of PCSBs.

2. Proposed model

The model described hereafter reproduces the test span of the SES in Bangkok [14]. This is one of the very few full-scale experimental models of PCSBs tested until failure under static loads. Additionally, other researches have also used this test span to validate their models [8,13,15,19,23], which would allow for comparison of the performance of the model.

The deck was a box girder 44.25 m long, spanning 43.25 m, and was divided in 14 segments. Fig. 1 shows a longitudinal section of the test span indicating the position of the segments, joints and tendons, and the

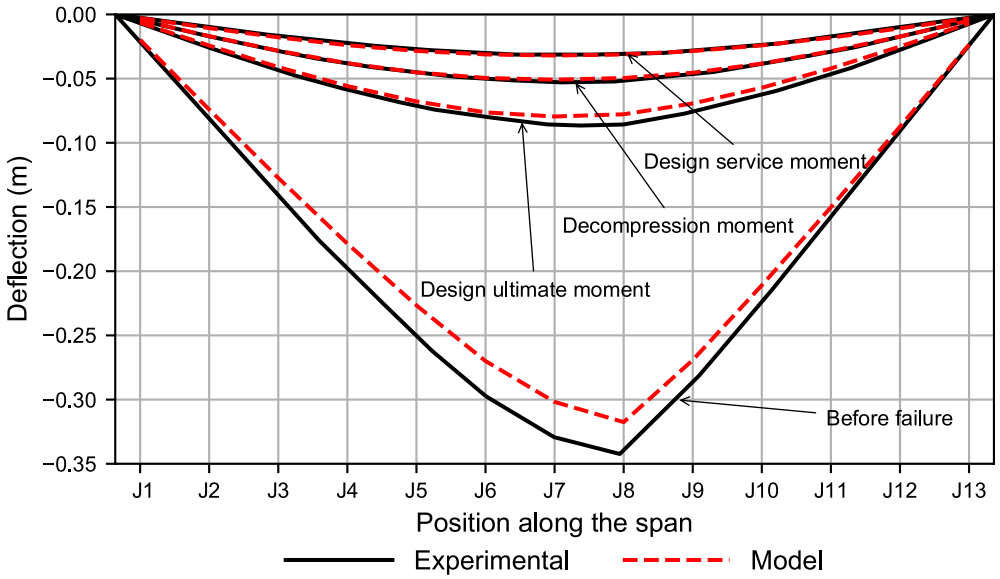

Fig. 6. Comparison of the deformed profile of the test span at different load levels obtained from the experimental results [14] and the proposed FE model.

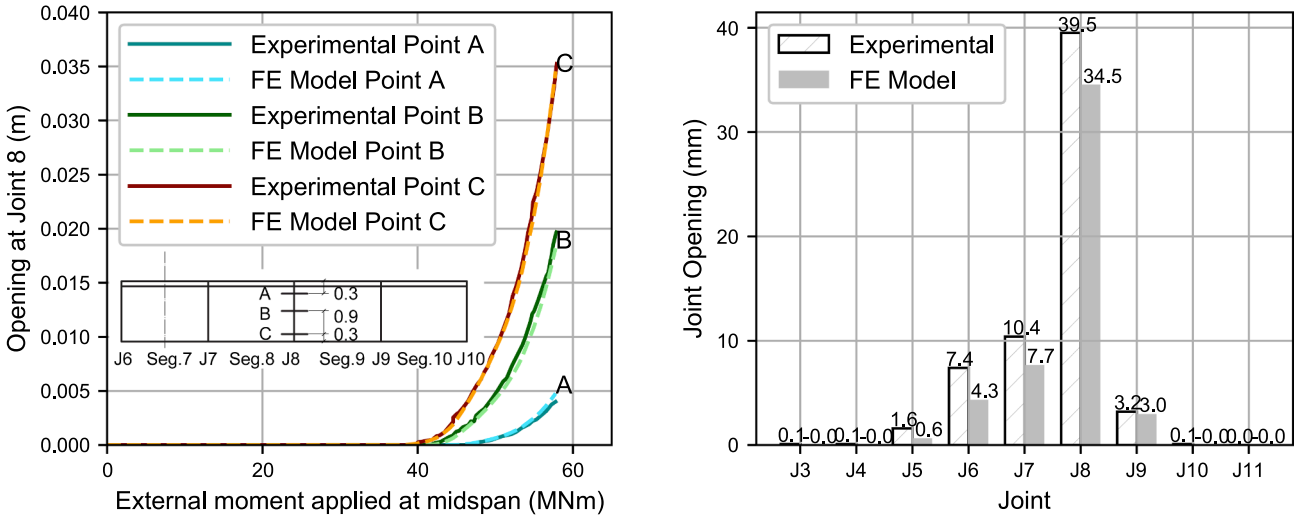

Fig. 7. Comparison of the joint opening of the critical joint (Joint 8) at different heights, left, and comparison of the distribution of joint openings at failure, right, for the experimental results [14] and the FE model.

cross section over the supports and at the central deviator. The joints between the segments were dry joints with shear keys. It used external post-tensioning with 6 pairs of tendons. All of them were protected by high density polyethylene (HDPE) sheaths and cement grout. The ducts were continuous through the deviators, with the HDPE sheath being in direct contact with the concrete [27].

The model has been created in ABAQUS 2018 [28]. The box girder is modelled using shell quadrilateral elements with reduced integration (S4R) [28] (Fig. 2). The average size of the elements is 0.25 m. It was chosen after a sensitivity analysis and allowed achieving good accuracy and convergence of the model at a reasonable computational cost. The diaphragms and deviators are also included in the model.

The tendons are modelled using quadratic beam elements (B31) [28] running between anchorages and deviators. Their area depends on the number of strands in each tendon, 12 or 19, and the area of each K15 strand: 140 mm^2. At the deviators, only the movement along a line on the plane defined by the two segments of tendon arriving at the deviator is free. This line is perpendicular to the bisector of those segments. This is done using the SLOT connector [28]. The friction coefficient between the tendon elements and the elements representing the deviator in the direction of the free movement is 0.15. This was the value adopted for the prestress losses at the deviators in the design of the SES in Bangkok [27]. Takebayashi et al. [14] however, measured the slip between the HPDE sheath and the deviator, which may be associated with a different friction behaviour. There is scarce information in the literature about the friction coefficient when slip happens between the deviator and the tendons. In an experimental study, Fouré and Hoang [29] measured values in the range of 0.14 to 0.19 for the case of a tendon within a HPDE sheath passing through a galvanized duct in the deviator. The value of 0.15 adopted is within this range, although when the HPDE sheath is in direct contact with concrete, a higher friction coefficient could be expected. The impact of the variability of this parameter is addressed in the analysis in Section 4.1.

Together with the weight of the bridge, the value of the prestressing force controls the global behaviour of the model [15], and more specifically, the load level that provokes the opening of the joints. The value of the prestressing force was thus calibrated to match the experimental results, accounting for prestress losses in a simplified manner. The

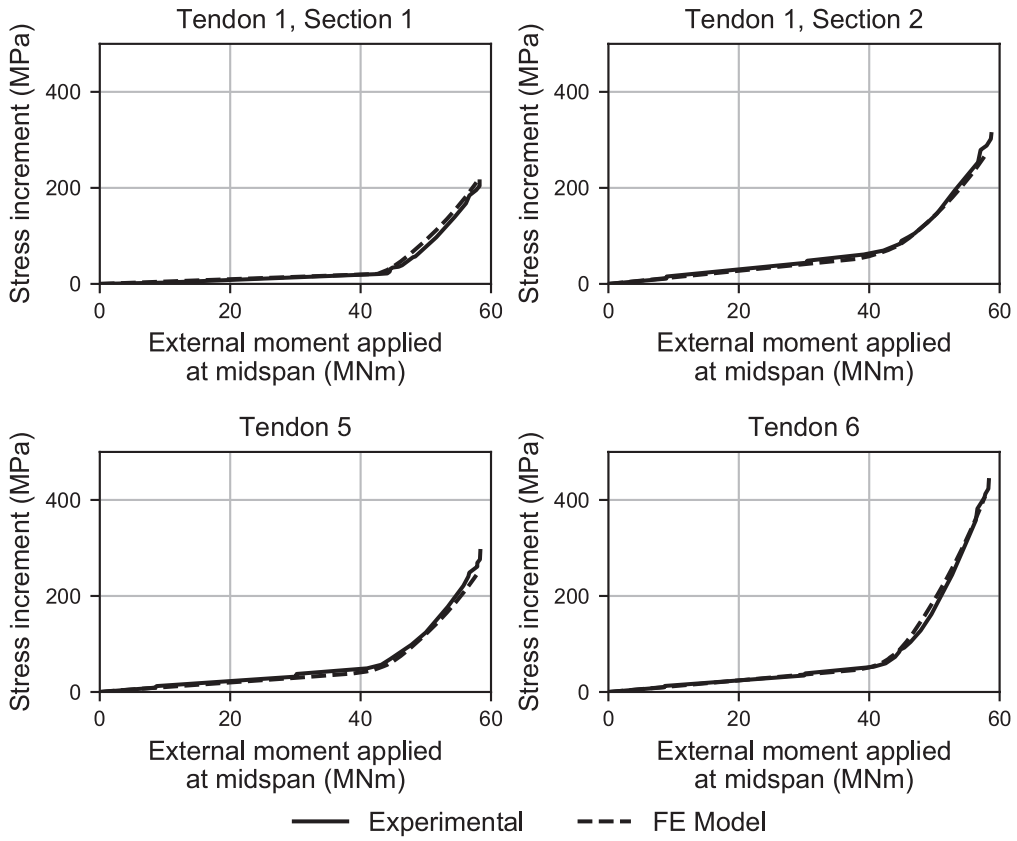

Fig. 8. Comparison of the stress increments in the tendons for the experimental results [14] and the FE model. Stresses in tendon 1 change significantly at both sides of the deviators (Section 1 between the left abutment and deviator 1, top left, and Section 2 between deviators 1 and 2, top right, see Fig. 1), whereas for tendons 5, bottom left, and 6, bottom right, stresses are considerably homogeneous for the whole length.

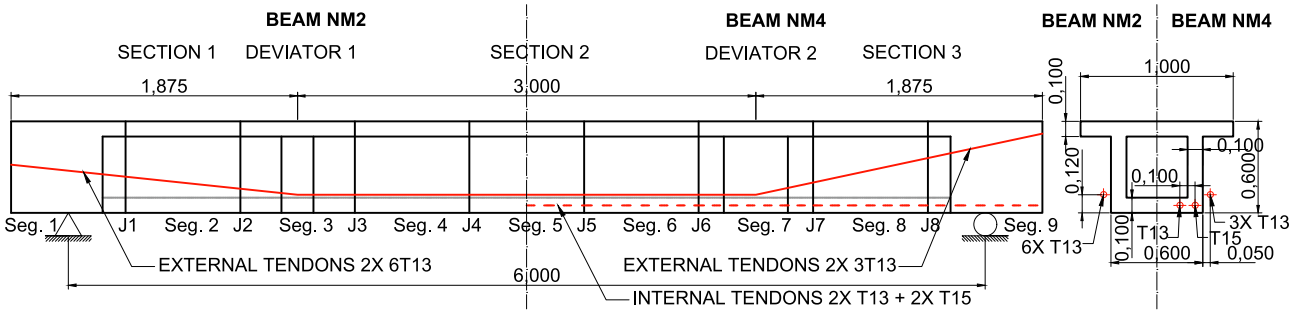

Fig. 9. Elevation view and cross section of beams NM2 (left half of the span) and NM4 (right half of the span), and cross section.

original jacking stress of 1435 MPa [27] was reduced by 12 % to account for the losses observed by Takebayashi et al. [14] and obtain an average stress in the prestressing tendons of 1263 MPa before the start of the test. The prestress applied is 1325 MPa to account for the elastic shortening of the model under the effects of the prestress and the dead loads.

The test load is introduced as a distributed surface load directed downwards applied on the areas of the top slab that were loaded in the original experiment [14]. Its magnitude is increased progressively until failure.

The behaviour of the reinforcement and prestressing steel is included in the model through simplified elastic–plastic laws defined following Eurocode 2 [30] and shown in Fig. 3. The von Misses yield criterion is used for both types of steel.

The mean strength of concrete and its Young's modulus take values of 55 MPa and 43 GPa respectively [14]. The behaviour of concrete is modelled as elastic up to 40 % of its mean strength. This is followed by a plastic branch with hardening until the peak stress is reached, after which a softening branch is included (Fig. 3).

This uniaxial behaviour law is used in the constitutive model for concrete available in ABAQUS 2018 [28]. The model defines a yield surface in compression and uses a smeared cracking approach for the concrete in tension accounting for tension stiffening. For this model to produce adequate results it is necessary to define the reinforcement carefully. To improve convergence of the model, cracking and failure in compression are only considered in the critical areas of the model, namely the top slab and the webs next to the joints.

The reinforcement is defined for the whole model with layers of steel embedded in the concrete shell elements. These layers are located on the reference surface of the shell elements.

The joints between the segments are modelled using node-to-node contact elements (GAP) [28] with null length and hard contact formulation. Friction at the joints follows a Coulombian friction model

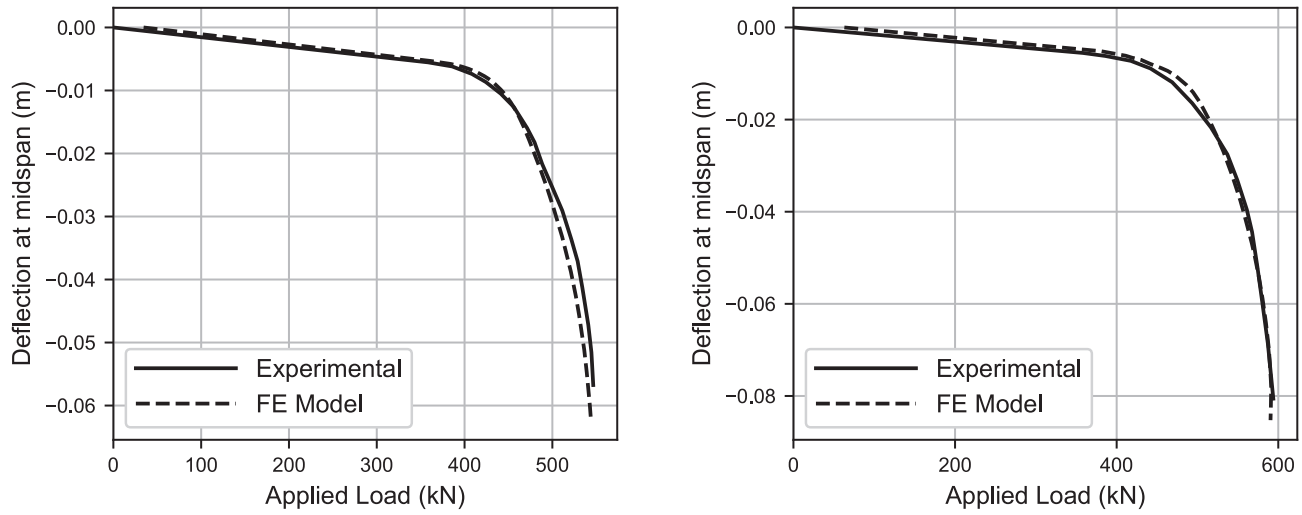

Fig. 10. Comparison of the deflection of Beam NM2 (left) and Beam NM4 (right) obtained from the experimental results [17] and the FE model.

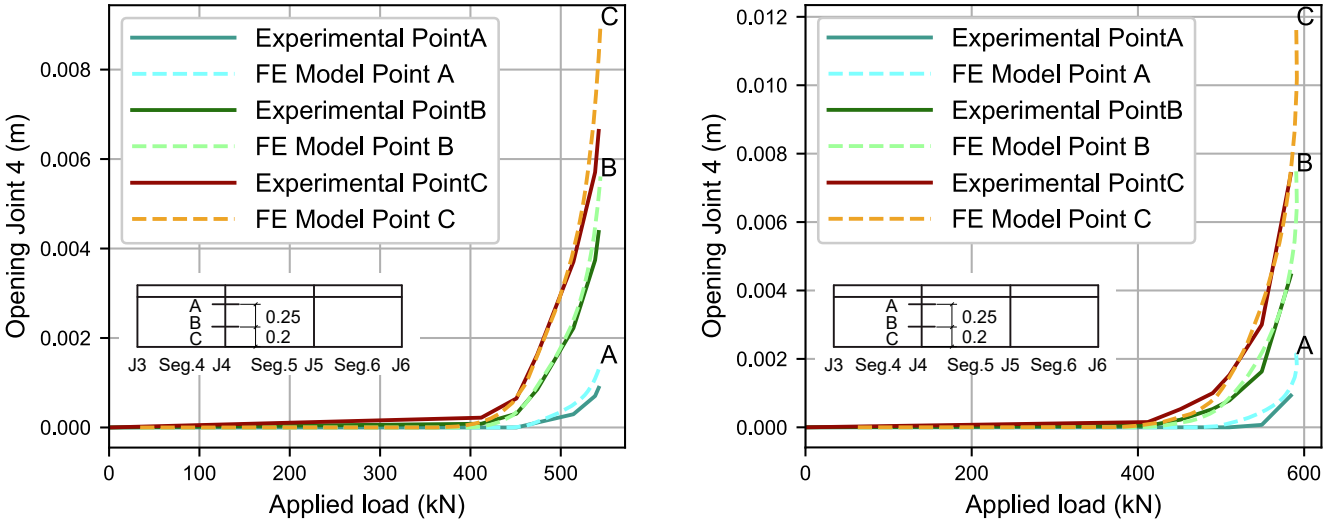

Fig. 11. Opening of the critical joint (Joint 4) at different heights for the experimental results [17] and the FE model for Beam NM2 (left) and Beam NM4 (right).

enforced through the penalty method and with a friction coefficient of 0.6, as adopted in previous research on numerical models for PCSBs [12,15,22]. For the bottom slab and the webs, the contact elements join directly the corresponding nodes of the meshes of the adjoining segments. For the top flange, which is expected to work in compression under the failure mechanism, two contact elements are used in the thickness of the slab for each node of the mesh of the segments, as shown in Fig. 4, above and below the reference surface of the shells. The final position of the contact elements is chosen after a sensitivity analysis.

3. Comparison with experimental results

3.1. Bangkok second stage expressway system test span

In general, the model shows very good agreement with the tests by Takebayashi et al. [14]. Fig. 5 compares the results from the test and the model in terms of deflection measured at the bottom of the left web at Joint 7 (Fig. 1) and applied moment during the load test. Fig. 6 compares the deformed profile from the test and the model under different load levels. The lack of symmetry of the deformed profile before failure is a result of the asymmetric location of the deviators with respect to the midspan section [14].

The model matches well the experimental stiffness both before and after the opening of the joints. The decompression load in the model (when the very first joint starts to open) corresponds to an applied moment of 37.7 MNm, which is close to the 36.5 MNm moment in the test (3.30 % difference). The external moment at failure measured in the test was 58.20 MNm while the model failed for a moment of 57.76 MNm at midspan (0.76 % difference). The displacement at failure was 0.325 m in the test and 0.302 m in the model (7.36 % difference).

The FE model matches well the experimental results in terms of opening of the critical joint (Fig. 7, left). Due to lack of data in the original paper describing the experimental test, the height of the measuring points for the joint opening was taken from Yuen et al. [15]. The maximum opening in the model is 34.5 mm while it was 39.5 mm in the test. The openings are more concentrated at the critical joint in the model (Fig. 7, right).

The FE model also matches well the stress increments in the tendons (Fig. 8), both when the effects of friction at the deviators are relevant and restrain slip, as is the case of tendon 1, and when slip prevails, such as in tendons 5 and 6. In general, the model follows well the test results in terms of slip at the deviators, although at some deviators it shows better agreement than at others, which could be attributed to differences in the friction behaviour at different deviators.

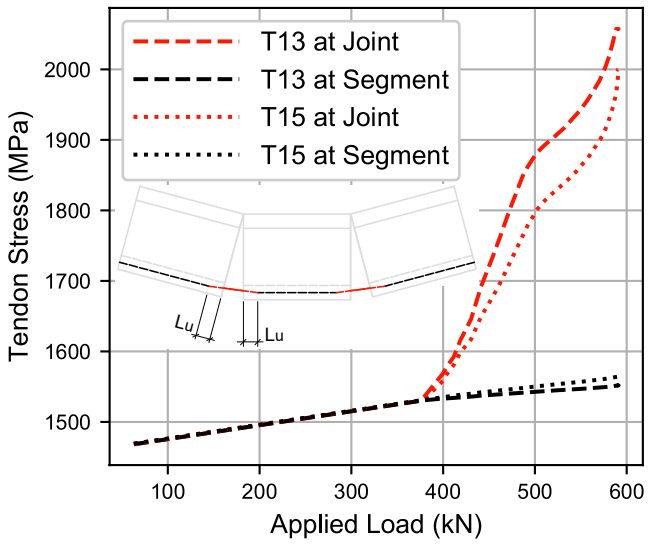

Fig. 12. Stress in the internal tendons of Beam NM4 under the action of the test load obtained from the FE model. In red, stresses of the tendons at the critical joint sections and in black, stresses at the mid-section of Segment 5. (For interpretation of the references to colour in this figure legend, the reader is referred to the web version of this article.)

Failure of the test span happened by crushing of the concrete of the top slab over the critical joint [14]. Similarly, in the FE model, failure happens when it is no longer possible to converge to a solution for the plastic behaviour in compression of the concrete elements of the top slab over the joint. Additionally, the model also shows cracking of the web elements next to the central joints of the span, which was also observed during the experimental tests [14]. If not enough reinforcement is provided in this area, the model fails prematurely before crushing of the top slab. In the model, cracking of the webs starts for an applied moment of 44.6 MNm, very close to the 45 MNm at which it was first observed in the test.

3.2. *Tests at the Centre d'Études du Bâtiment et des Travaux Publiques*

The numerical model developed herein for the SES test span has been adapted to reproduce the results of the experimental tests developed by Fouré et al. [17] on precast concrete segmental beams at the Centre d'Études du Bâtiment et des Travaux Publiques (CEBTP).

Fouré et al. [17] conducted a series of tests on a total of 11 beams, 5 of which were segmental beams with dry joints and 6 monolithic, with different types of prestressing: internal, external or both, and different reinforcement ratios. The beams were tested until failure measuring data on their global behaviour, opening of the joints, cracking and failure modes, and obtaining some information about the tension in the prestressing tendons. Only two of those 11 specimens have been studied in this work, the segmental beams named NM2 and NM4. The beam NM2 has only external draped tendons, while beam NM4 combines both external draped tendons and straight internal tendons (Fig. 9).

The segmental beams are 6.75 m long, spanning 6 m and composed of 9 segments of 0.75 m each [17]. The two end diaphragms cover the whole section and are 0.6 m thick.

The external tendons of both beams have a draped profile with the central section between deviators parallel to the bottom surface of the top slab at a theoretical distance of 0.12 m. Additionally, beam NM4 has two pairs of straight internal tendons. All the external tendons are placed in corrugated metallic sheaths injected with cement. The sheaths are continuous through the deviators passing by steel tubes. The internal tendons are placed in steel tubes with smooth surface and injected in cement. Fouré et al. [17] provide the value of the measured force in the prestressing tendons at the beginning of the load test. The beams are loaded symmetrically with two point loads applied on top of the intermediate deviators.

The numerical model for beam NM2 follows the same strategies as those for the SES test span. The only significant difference affects the stress–strain relationship used for the prestressing steel. In this case, since the stresses in the tendons exceeded the yielding point during the tests, the behaviour of the prestressing steel is taken linear up to 80 % of the breaking strength of the tendon and then follows the "Power Formula" as proposed by Mattock [31]. The average strength of concrete is taken as 45.7 MPa and its Young's modulus is 36.2 GPa. The yield strength of the reinforcement steel is 475 MPa.

For the numerical model of beam NM4, the internal tendons are modelled with beam elements (B31) [28]. They are joined to the mesh representing the concrete section at every node and constrained to have the same displacements. However, the tendons are not linked to the concrete for a certain length in the vicinity of the joints to reproduce the effect of debonding of the tendons at the joints. This distance has been taken equal to the tendon equivalent unbonded length (L_u) as defined by Veletzos and Restrepo [10].

The results from the model have been compared with the data obtained by Fouré et al. [17]. Fig. 10 compares the deflection history from the FE model with the experimental test.

The results in terms of opening of the critical joint (Joints 4 and 5) from the FE model also show good agreement with the experimental test (Fig. 11), although the opening at failure load is slightly overestimated, which is related to the overestimation of the ultimate displacements in the model.

Fouré et al. [17] do not report the stress increment in the internal tendons. It is only mentioned that, considering that the external tendons suffer smaller stress increments in the case of beam NM4, internal tendons are probably concentrating the increment of stress. Fig. 12 shows very important differences between sections located at the joints and those within the segments. At the joint section, the stresses in the tendons increase rapidly after opening of the joints. Therefore, it is paramount to set up a model that includes the joints when modelling PCSBs to have an accurate estimation of the forces in the internal tendons.

4. Parametric studies

4.1. *Influence of friction at the deviators*

Choosing a different friction coefficient within the range of practical values only affects slightly the global behaviour of the models. The stiffness of the girder after the opening of the joints changes, increasing or decreasing in parallel with the friction coefficient (Fig. 13 top). Even if friction is completely ignored at the deviators, allowing for free slip of the tendons, the global behaviour (deflections and joint openings) does not change excessively. However, allowing free slip at the deviators has a strong impact on the stress increase in the different segments of the tendons (Fig. 13 bottom). The changes in behaviour are more relevant for those tendons with higher deviation angles such as Tendon 1 of the SES test span, as also observed by Takebayashi et al. [14], for which the normal and friction forces that appear at the deviator are bigger. Hence, it would be necessary to take into account friction to obtain appropriate estimates of the stress levels in the tendons. If full fixity of the tendons at the deviators is considered, the behaviour changes significantly. The stiffness of the girder after opening of the joints is much higher and so is the applied moment at failure. No redistribution of stresses happens in this case between the different segments of the tendons. The variation in the friction coefficient also affects the load level for which slip happens at the deviators. For lower values of the friction coefficient, slip starts earlier.

4.2. *Influence of the joint model*

The joints in the models do not include the shear keys, following the

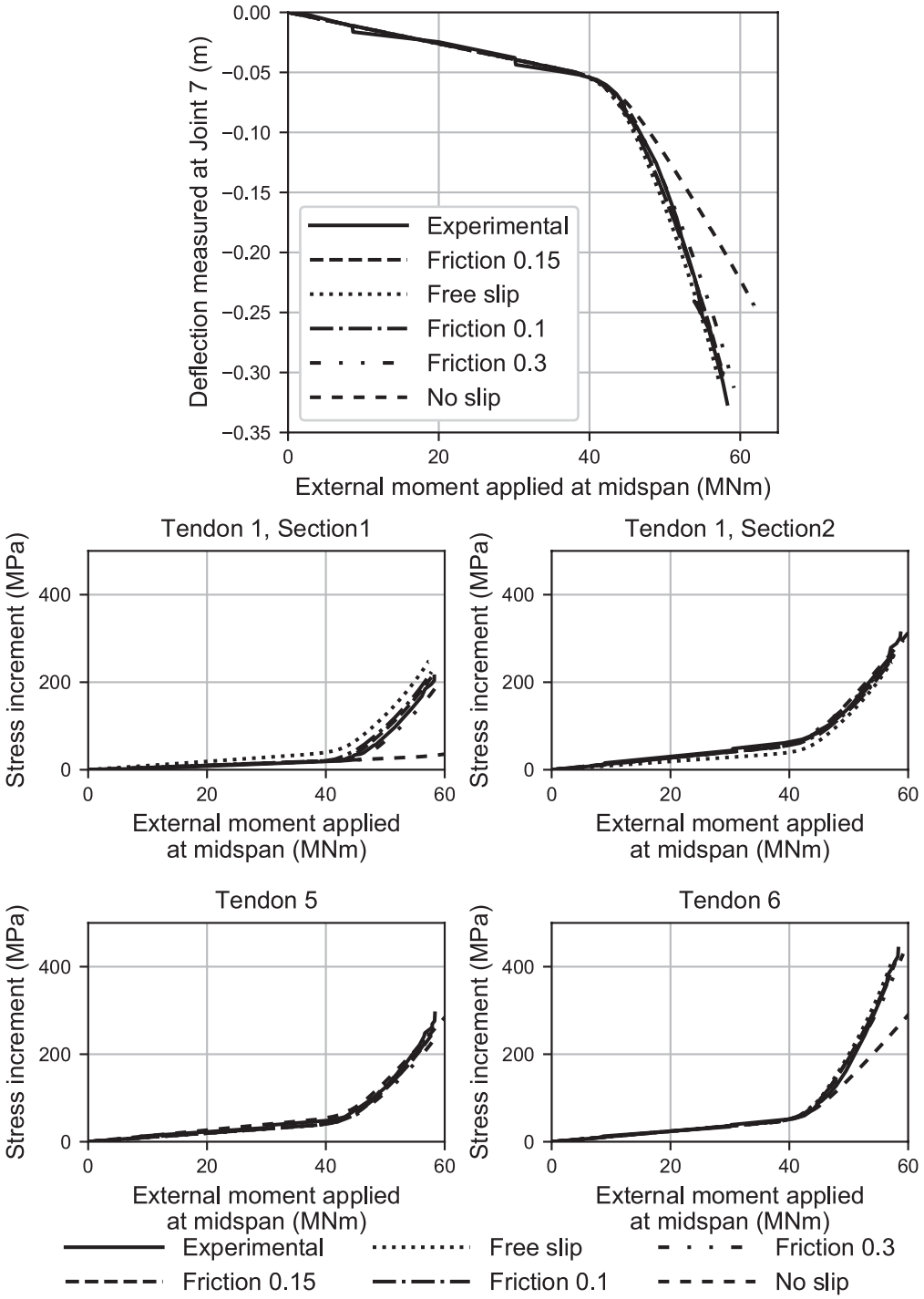

Fig. 13. Comparison of the deflection of the SES test span (top) and the stress increments in the tendons (bottom) obtained from the experimental results [14] and the FE model with a friction coefficient of 0.30, 0.15, 0.10, free slip or no slip allowed at the deviators.

conclusions of the previous works by Turmo et al. [11] and Specker and Rombach [13]. Since minimal sliding is observed, neglecting the contribution of the shear keys should not have a strong impact on the results. Moreover, changing the friction coefficient between the joint surfaces does not significantly affect the results of the models for values as low as 0.2, as shown in Fig. 14.

The modelling approach for the top slab has a strong influence on the behaviour of the model after opening of the joints. If the joints between the segments are modelled with a single layer of contact elements at the top flange, when the opening of the critical joint reaches the top slab the girder starts rotating around the joint, which behaves as a hinge (Fig. 15). Moreover, it is not possible to transfer bending moments acting at the top flange across the joint in the top slab, which affects the distribution of stresses. With two contact elements, it is possible to transfer the moments acting at the shell elements of the top slab across the joints, and the sudden formation of a hinge at the joint is prevented. The height of the elements above the reference surface affects the stiffness after the opening of the joints, since it determines the depth between the prestressed tendons and the concrete in the top slab. Additionally, when the position of the contact element is higher the rotation radius increases

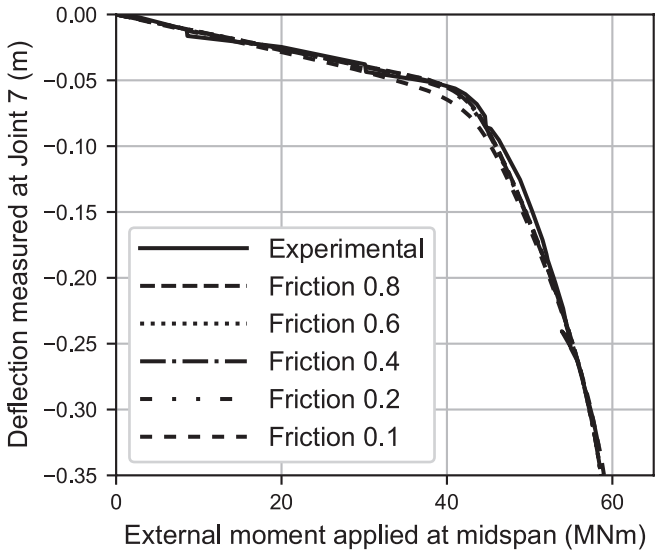

Fig. 14. Comparison of the deflection of the test span obtained from the experimental results [14], and the proposed FE model with different values of the friction coefficient at the joints.

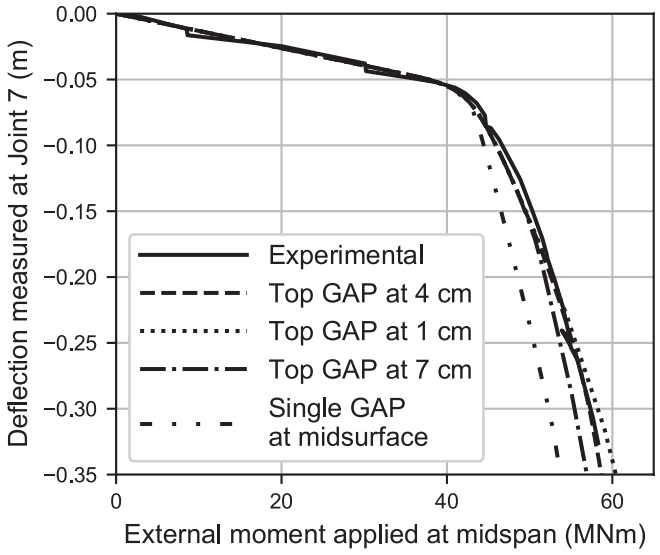

Fig. 15. Deflection of the SES test span when the contact element above the reference surface is located at 4, 1 and 7 cm from the top surface of the top slab and with a single contact element at the reference surface.

and the opening of the joint is smaller.

Estimating a priori the position of the top contact element is difficult due to the absence of deformation compatibility at the joint. A possible estimation could be given by the height of the resultant of compression forces through the joint at the top slab. Similarly to the proposal for estimating the stress increment in unbonded tendons by MacGregor et al. [3], both the tendons and the concrete may be assumed to attain their respective yield stresses. With this assumption, and neglecting the effects of shear lag, the point of application of the compressive resultant in concrete would be at 4.6 cm from the surface of the top slab. This value is close to the 4 cm that was found to be the position of the top contact element best matching the experimental results (Fig. 15). Therefore, this simple approach can be used to determine the location of the top contact element in other cases.

The results from the model with two contact elements at the top slab were compared with a model where the top slab is modelled with solid

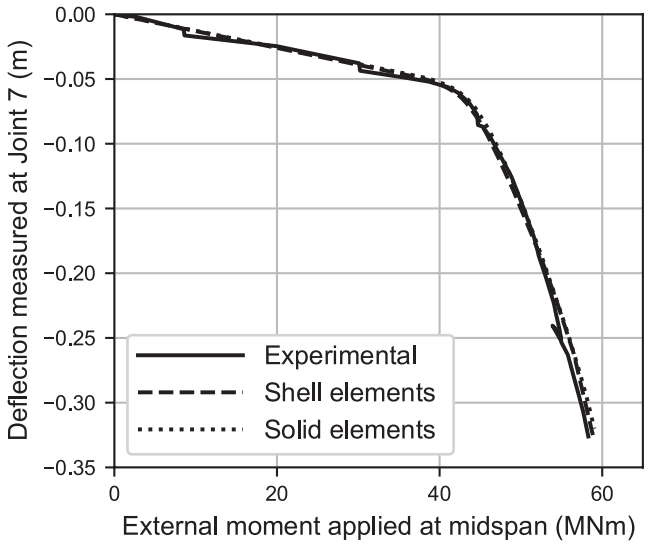

Fig. 16. Comparison of the deflection of the SES test span obtained from the experimental results [14] and the FE model with shell or solid elements at the top slab.

elements (Fig. 16). Both models show good agreement with the experimental results and very similar global behaviour of the test span.

Some differences exist in the stress distribution between the two models. In the model with solid elements in the top slab, the elements located in the bottom face of the top slab are not in contact when the joint opens and thus do not transfer any normal stress. In the model with shell elements however, even if the contact elements located below the reference surface of the top slab are not in contact, the whole shell element reacts to the forces transmitted through the top contact element. Hence, compression stresses appear on the top face of the element and tension stresses at the bottom face, unless prevented by the cracking of concrete. Fig. 17 compares the longitudinal stresses at the top and bottom fibres of the top slab over the critical joint (Joint 8). The models with shell elements accounting for cracking of concrete and with solid elements at the top slab show similar behaviour, while the model with shell elements and plastic behaviour provides different results mainly due to the tension stresses appearing at the bottom fibre. It must be noted that the use of the model with shell elements instead of solid elements in the top slab reduces the computation time by a factor of 17.

4.3. *Influence of the equivalent unbonded length*

The model of the beam NM4 tested at the CEBTP adopted the concept of equivalent unbonded length as proposed by Veletzos and Restrepo [10] to reproduce the behaviour of internal tendons at the joint sections. Their proposed formulation estimates the equivalent unbonded length proportional to the square root of the area of the tendons.

The stresses in the internal tendons at the open joint increase significantly in comparison to the stresses in those tendons once the bonding is guaranteed. The smaller the unbonded length affected by the joint opening, the larger the stress increment (Fig. 18 right).

As the equivalent unbonded length increases, the model loses stiffness faster after the opening of the joints (Fig. 18 left). The larger loss of stiffness for longer unbonded lengths is expected, since when this length increases the tendons become more deformable at the joints. Good results are obtained using the formulation by Veletzos and Restrepo [10].

4.4. *Influence of epoxy at the joints*

An adapted version of the model of beam NM4 has been employed to analyse the influence of introducing a layer of epoxy at the joints. In this new model of beam NM4, spring elements (Axial Connectors) [28] with

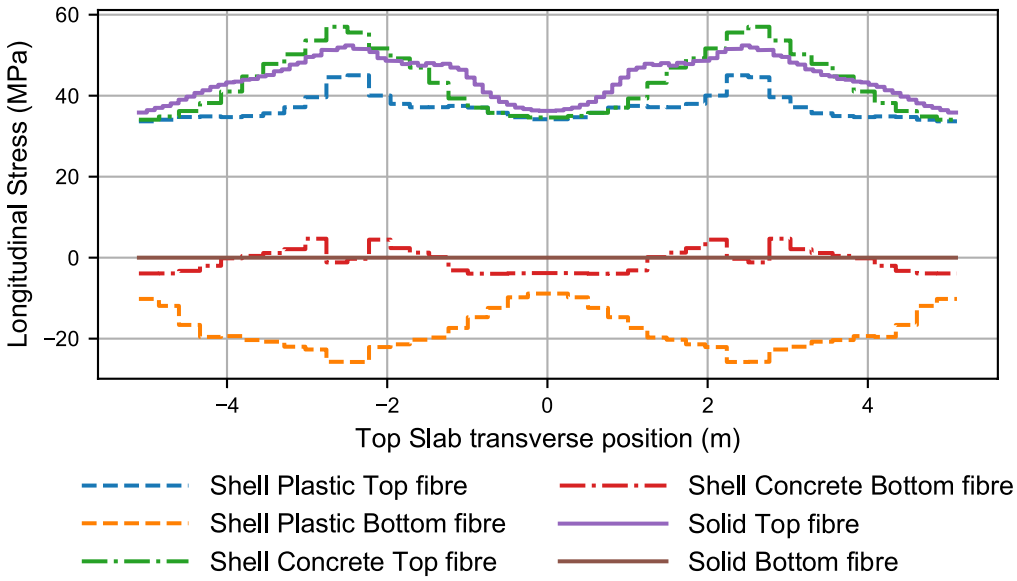

Fig. 17. Longitudinal stresses in the top slab of the SES test span at Joint 8 for an external applied moment of 56.5 MNm for a model with shell elements and considering cracking and failure of concrete in the top slab and the web next to the joints, for a model with shell elements and simplified plastic behaviour and for a model with solid elements at the top slab. Compression stresses are depicted positive and tension stresses negative.

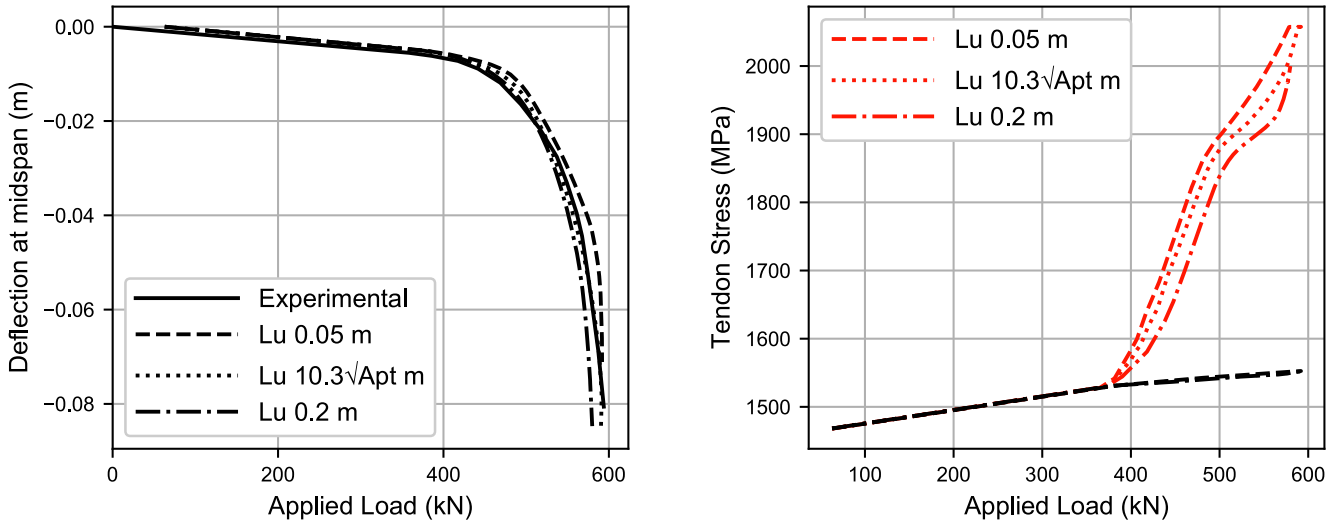

Fig. 18. Comparison of the deflection (left) and the stress in the internal tendons (right) of Beam NM4 obtained from the experimental results [17] and the FE model considering an equivalent unbonded length for internal tendons at the joints of 0.05 m, the length defined by Veletzos and Restrepo (0.1 m), and 0.2 m.

non-linear behaviour and zero initial length have been added between the nodes of the segments in contact (except in the top slab), in parallel with the contact elements, to model the effect of the epoxy layer. To consider cracking, damage behaviour is implemented for the springs, starting at the load corresponding to the tensile capacity of the adjacent concrete.

In Fig. 19, it can be appreciated that the curves for the two models only differ slightly at the stiffness transition zone when the joints open. The model with epoxied joints shows a more sudden change in stiffness. This is related to the sudden release of energy when the concrete cracks next to the epoxy joints [32]. These results, showing very similar behaviour, and the higher complexity implied by considering epoxied joints in the model, may justify not considering the epoxy layer in future models of PCSBs.

5. Conclusions

A FE model has been presented reproducing the behaviour Precast Concrete Segmental Bridge decks. The model accounts for the opening of the joints, the friction of external tendons at the deviators, and the combination of internal and external tendons. Moreover, the effect of the epoxy layer at the joints has been analysed.

The results from the model show good agreement with the experimental results, reproducing accurately the change of behaviour when the joints open, the evolution of the opening of the joints and the stress increase in the tendons until failure.

The influence of some of the modelling choices such as the model for the joints has been studied. It was shown that the modelling strategy used for the top slab had a strong impact on the behaviour of the FE model. The use of shell elements at the top slab with two contact elements at the joints showed improved accuracy, comparable with that obtained with a more complex model with solid elements at a much

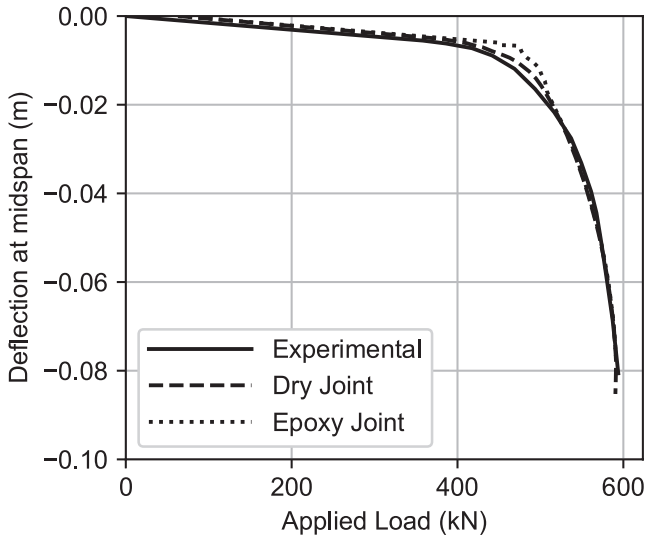

Fig. 19. Comparison of the deflection of Beam NM4 obtained from the experimental results [17] and the FE model considering dry and epoxied joints.

lower computational cost (1/17th), and better than in models using shell elements with a single contact element at the top slab. With this modelling strategy for the joints, it was found that the stiffness after the joints had opened was determined mainly by the height of the top contact element at the top slab. The model with simplified plastic behaviour for concrete provided good results in terms of global deflections and might be suitable for certain analysis, but it is not accurate enough to represent stresses in the section and failure.

Additional modelling strategies have been adopted for the inclusion of internal bonded tendons in the model and for the consideration of the epoxy layer at the joints. This allows extending the range of application of the models to cover the typologies of PCSB decks most commonly employed in the construction industry. The results point out to a limited influence of the epoxy layer on the global structural behaviour of PCSB decks.

The accuracy of the models presented in this paper to represent the geometric and mechanical characteristics and the static behaviour of the decks in PCSBs at a reasonable computational cost, makes them suitable candidates for more complex analyses and to study the dynamic behaviour of these type of bridges as part of a future research.

CRediT authorship contribution statement

Javier Cañada Pérez-Sala: Methodology, Investigation, Writing – original draft, Visualization. **Ana M. Ruiz-Teran:** Conceptualization, Writing – review & editing, Supervision.

Declaration of Competing Interest

The authors declare that they have no known competing financial interests or personal relationships that could have appeared to influence the work reported in this paper.

Data availability

Data will be made available on request.

References

[1] Combault J. Design and construction of segmental bridges for high speed rail. ASPIRE 2013:18–21.
[2] Rettinger M, Hückler A, Schlaich M. Technologien und Entwicklungen im Segmentbrückenbau. Beton- Stahlbetonbau 2021;116:12–23. https://doi.org/10.1002/best.202100054.
[3] Macgregor RJG, Kreger ME, Breen JE. Strength and ductility of a three-span externally post-tensioned segmental box girder bridge model; 1989.
[4] Virlogeux M. New trends in prestressed concrete bridges. Struct Concr 2002;3:67–97. https://doi.org/10.1680/stco.2002.3.2.67.
[5] Clark GM. Post-tensioned structures – improved standards. Proc ICE - Forensic Eng 2013;166:171–9. https://doi.org/10.1680/feng.13.00010.
[6] Yuan A, He Y, Dai H, Cheng L. Experimental study of precast segmental bridge box girders with external unbonded and internal bonded posttensioning under monotonic vertical loading. J Bridg Eng 2015;20:1–12. https://doi.org/10.1061/(ASCE)BE.1943-5592.0000663.
[7] Ramos G, Aparicio ÁC. Ultimate analysis of monolithic and segmental externally prestressed concrete bridges. J Bridg Eng 1996;1:10–7. https://doi.org/10.1061/(ASCE)1084-0702(1996)1:1(10).
[8] Yan WT, Han B, Xie HB, Li PF, Zhu L. Research on numerical model for flexural behaviors analysis of precast concrete segmental box girders. Eng Struct 2020;219:110733. https://doi.org/10.1016/j.engstruct.2020.110733.
[9] Veletzos MJ, Restrepo JI. Modeling of jointed connections in segmental bridges. J Bridg Eng 2011;16:139–47. https://doi.org/10.1061/(ASCE)BE.1943-5592.0000112.
[10] Veletzos MJ, Restrepo JI. Equivalent unbonded length for modeling of multistrand tendons in precast segmental construction. J Bridg Eng 2014;19:101–9. https://doi.org/10.1061/(ASCE)BE.1943-5592.0000502.
[11] Turmo J, Ramos G, Aparicio ÁC. FEM modelling of unbonded post-tensioned segmental beams with dry joints. Eng Struct 2006;28:1852–63. https://doi.org/10.1016/j.engstruct.2006.03.028.
[12] Turmo J, Ramos G, Aparicio ÁC. FEM study on the structural behaviour of segmental concrete bridges with unbonded prestressing and dry joints: simply supported bridges. Eng Struct 2005;27:1652–61. https://doi.org/10.1016/j.engstruct.2005.04.011.
[13] Specker A, Rombach GA. Ein beitrag zur konstruktion und bemessung von segmentbrücken. Beton- Stahlbetonbau 2001;96:654–62. https://doi.org/10.1002/best.200100840.
[14] Takebayashi T, Deeprasertwong K, Leung YW. A full-scale destructive test of a precast segmental box girder bridge with dry joints and external tendons. Proc Inst Civ Eng - Struct Build 1994;104:297–315. https://doi.org/10.1680/istbu.1994.26780.
[15] Yuen TYP, Halder R, Chen WW, Zhou X, Deb T, Liu Y, et al. DFEM of a post-tensioned precast concrete segmental bridge with unbonded external tendons subjected to prestress changes. Structures 2020;28:1322–37. https://doi.org/10.1016/j.istruc.2020.09.080.
[16] Halder R, Yuen TYP, Chen WW, Zhou X, Deb T, Zhang H, et al. Tendon stress evaluation of unbonded post-tensioned concrete segmental bridges with two-variable response surfaces. Eng Struct 2021;245:112984. https://doi.org/10.1016/j.engstruct.2021.112984.
[17] Fouré B, Rezende Martins P, Hoang LH. Problèmes de sécurité à rupture et de modélisation du comportement des poutres en béton à précontrainte extérieure. Ann l'ITBTP 1991;491:46–95.
[18] Huang J, Eibl J. Design of Segmental Bridges under Combined Bending, Shear and Torsion FE-Study. In: Conti E, Fouré B, editors. Extern. Prestress. Struct. Proc. Work. Behav. Extern. Prestress. Struct., Saint-Rémy-Lès-Chevreuse: Association Française Pour la Construction; 1993, p. 335–47.
[19] Tandler J. Collapse analysis of externally prestressed structures; 2001.
[20] Megally SH, Garg M, Seible F, Dowell RK. Seismic performance of precast segmental bridge superstructures with internally bonded prestressing tendons. PCI J 2002;47:40–56.
[21] Da Silva RA, Rodrigues Pacheco A, Campos FA. Finite element analysis of segmental concrete bridges. Bridg Struct 2005;1:257–71. https://doi.org/10.1080/15732480500256398.
[22] Jiang H, Deng Y, Qiu Y, Wei C, Chen L, Feng W. Numerical analysis of mechanical properties of precast segmental concrete test beam with external tendons. Adv Mater Res 2013;639–640:460–9. https://doi.org/10.4028/www.scientific.net/AMR.639-640.460.
[23] Sejkati E, Zhou X, Shamass R, Mancini G. Modelling post-tensioned precast concrete segmental girger bridges with keyed joints - preliminary results. In: Proc 9th Int Concr Conf 2016 Environ Effic Econ Challenges Concr, Springer Verlag; 2016, p. 13.
[24] Lazzari PM, Filho AC, Lazzari BM, Pacheco AR. Structural analysis of a prestressed segmented girder using contact elements in ANSYS. Comput Concr 2017;20:319–27. https://doi.org/10.12989/cac.2017.20.3.319.
[25] Virlogeux M, M'Rad A. Flexural behaviour of externally prestressed structures for ultimate loads. In: Conti E, Fouré B, editors. Extern. Prestress. Struct. Proc. Work. Behav. Extern. Prestress. Struct., Saint-Rémy-Lès-Chevreuse: Association Française Pour la Construction; 1993, p. 185–206.
[26] Naaman AE, Alkhairi FM. Stress at ultimate in unbonded post-tensioning tendons. Part 2. Proposed methodology. ACI Struct J 1991;88:683–92. <https://doi.org/10.14359/1288>.
[27] Hewson NR. Use of external tendons for the Bangkok second stage expressway. Struct Eng 1993;71:412–35.
[28] Dassault Systèmes. ABAQUS; 2018.
[29] Fouré B, Hoang LH. Experimental study of the local behaviour of cables and sheath inside the deviators. In: Conti E, Fouré B, editors. Extern. Prestress. Struct. Proc. Work. Behav. Extern. Prestress. Struct., Saint-Rémy-Lès-Chevreuse: Association Française Pour la Construction; 1993, p. 97–107.

[30] CEN European Committee for Standardization. Eurocode 2: Design of concrete structures — Part 1-1: General rules and rules for buildings 2015:226. <https://doi.org/10.7773/cm.v27i4.501>.

[31] Mattock AH. Flexural strength of prestressed concrete sections by programmable calculator. PCI J 1979;24:32–54. https://doi.org/10.15554/pcij.01011979.32.54.

[32] Ramírez AG. Behavior of Unbonded Post-Tensioning Segmental Beams with Multiple Shear Keys.pdf. University of Texas at Austin 1989.